Wind pressure on surfaces of low-rise buildings

Prof. H. J. Gerhardt, M. Sc.; Prof. Dr.-Ing. C. Kramer*

A comprehensive investigation was undertaken to determine the wind pressures on surfaces of models of typical low-rise buildings. For many practical applications building surfaces like façade coverings or tiled roofs are permeable. For those coverings the pressure equilibration across the permeable surface is important when determining the net windload. A survey of the physical parameters influencing the windload of permeable surface coverings will be given. Results of a continuing study of the windload on permeable façade coverings will be presented.

1.0 Introduction

Over the past ten years the windload on low-rise structures has been extensively investigated at the Fluid Mechanics Laboratory of the Fachhochschule Aachen. The importance of such studies is evident from the amount of damage occuring even at moderately strong winds in particular on flat roofs, tiled inclined roofs and on wall claddings of low-rise structures. Research thus far has been mainly concerned with the windload on the external, impermeable walls of such buildings (see e. g. ref. 1, 2, 3). This paper surveys the essential physical parameters influencing the windload of permeable surface coverings. Some practical applications of the results obtained from wind-tunnel tests will be discussed.

* Fluid Mechanics Laboratory, Fachhochschule Aachen

2.0 Windloading mechanism

Windloads on a cladding or a roofing element are created by the difference of the external and the internal pressure. Here the internal pressure denotes the pressure in the space between external, permeable surface covering and the wind impermeable building surface. As shown schematically in fig. 1, taken from (4) the net windload is determined by the building flow field, the wind gustiness and the element flow field. While these parameters influence directly the external pressure distribution on the cladding or roofing elements the development of the internal pressure depends only indirectly on these parameters and is governed by dynamic response functions. The dynamic response functions differ for various cladding or roofing elements. Typical cladding elements include curtain walls, concrete, metal or asbesto-cement panels; typical roofing elements include tiles, paving blocks and sealing membranes. In this paper first results of an ongoing investigation concerning the windload on typical ETERNIT-cladding elements will be presented. Data obtained from windtunnel tests on roofing elements will be published elsewhere.

3.0 Windloading on façade elements

Windloading codes are usually based on windtunnel studies on building models with wind impermeable outer surfaces. Investigations into the windloading of wind permeable building surfaces were up to now only concerned with permeable roofing systems (4, 5). The highest windloads acting on building façades occur in regions of separated flow. The influence of the element flow field on the design windloads of façade elements and their fixations is therefore only of minor importance. The highest local windloads on relatively low-rise, sharp-edged buildings are obtained in low turbulence wind conditions (1, 6). Thus the results presented in this paper are based on measurements in smooth windtunnel flow. The influence of simulated atmospheric boundary layer conditions on the windloads of façade elements will be determined during the second part of the still ongoing

research program. For low turbulence windtunnel flow conditions, the net windload on façade elements will be mainly determined by the building flow field, see fig. 1.

3.1 Wind permeability of cladding systems

The response behaviour, fig. 1, which for a given external pressure distribution determines the pressure distribution in the space between a wind permeable façade covering and the wind impermeable building surface is governed by the wind permability of the façade covering. The variation of volume-flow through the façade coverings with the difference between external and internal pressure will be taken as a measure of the wind permeability. The volume-flow vs. pressure differential has been measured in full scale for various typical cladding systems. Fig. 2 gives some results. The pressure differential has been convieniently non-dimensionalized by the wind stagnation pressure q_∞ = 800 N/m² which is the design wind stagnation pressure for buildings of height H = 8 m ÷ 20 m according to the German Code of Practice DIN 1055, Bl. 4. The volume-flow $\dot{V}$ has been non-dimensionalized accordingly by the area A_D considered and the design wind speed U_∞ = 35,8 m/s. For the cladding elements thus far investigated the pressure differential is a parabolic function of the volume-flow, thus leading to straight lines in the chosen log, log-plot. The two different slopes recognisable for all systems correspond to laminar and turbulent flow conditions respectively in the gaps of the façade coverings. The basis for the design windloads are the largest pressure differences across the cladding elements leading to a turbulent flow situation in the gaps. For this flow situation the relation between pressure differential and volume-flow can be given as

$$c_p = C_D \cdot \alpha^2$$

The constant C_D is a measure for the wind permeability of the façade systems and depends directly on the percentage open area:

$$A_L/A_D = 1/\sqrt{C_D + 1}$$

With A_L = total effective cross section area of the gaps. For the usually sharp edged façade elements the geometric cross-section area has to be multiplied by the contraction number $\mu \approx 0{,}7$ to account for the vena contracta effect.

Fig. 3 shows the wind permeablility coefficient C_D for the façade elements considered in fig. 2. The results agree well with data given elsewhere (7). The model façades - perforated sheet metal plated with c_p, α-characteristics equivalent to the full-scale cladding elements - cover the relevant range of wind permeabilities. For comparison the wind permeability range of concrete tiles and clay tiles has been added.

3.2 Wall pressures

All measurements the results of which are reported in this paper were conducted in the Göttingen-type windtunnel of the Fluid Mechanics Laboratory of the Fachhochschule Aachen. The width of the octogonal nozzle is 1.1 m; maximum velocity U_∞ = 40 m/s. The building flow field around sharp-edged buildings is mainly influenced by the relative building dimensions: length/width ratio (L/B) and height/width ratio (H/B). Building models with the following relative dimensions have been investigated:

H/B = 0.25; 0.5; 1; 1.5 for L/B = 1; 2 respectively.

The side walls of the building models were provided with numerous pressure tabs, which could be connected via tubes either with a scani-valve or with a manometer-bank. The external pressure distributions were obtained from measurements on the six models with wind impermeable walls. All building models could be fitted with model façades of various permeabilities such as to enable the measurement of the internal pressure distributions.

3.2.1 External pressure distribution

The external pressure distribution on the wind impermeable smooth walls of the building models has been measured for wind direction parallel to the main axis of the building. From the pressure distribution mean external pressure coefficients have been calculated which can be compared with data given elsewhere (8, 9, 10). Fig. 4 gives the external pressure coefficient $\overline{c_p}$, ex vs. the relative building height for buildings with rectangular plane form. In particular for the long sides of the building the mean external pressure coefficient increases greatly with increasing relative building height. The rather large scatter of the data taken from the various references may be due to different edge contours of the buildings and different flow conditions. The main influence parameters will probably be the relative boundary layer thickness δ/H and the amount of small scale turbulence present in the oncoming flow. It may be assumed that the windload on permeable façade coverings will be far less dependent on the edge contours, the boundary layer thickness and the turbulence intensity of the oncoming flow since the external and the internal pressure distributions will be similarely influenced by these parameters.

All studies of the external pressure distribution thus far mentioned were concerned with wind impermeable façades of smooth building models. Wind permeable cladding systems are often rough. The influence of the surface roughness on the external pressure distribution of sharp-edged buildings has been extensively investigated by Vermeulen and Visser (11). The model façade coverings were chosen in such a way as to fullfil the two similarity criteria pointed out by Vermeulen and Visser.

3.2.2 Internal pressure distribution

The internal pressure distribution in the space between wind-permeable façade coverings and wind impermeable building wall will be mainly influenced by the external pressure distribution, the wind permeability of the façade coverings and the distance

between façade covering and building wall. The influence of the cladding distance from the building wall on the windload of the cladding elements has been investigated using a building model with the relative dimensions H/B = 0.25 and L/B = 1 for two typical wind permeabilities, fig. 5. For a large wind permeability the internal pressure distribution is similar to the external pressure distribution. The larger the relative distance between the cladding elements and the building wall (s/B) the better the agreement between internal and external pressure distribution. Air, leaving the space between cladding and building wall in regions of high external suction due to the negative pressure difference between external and internal pressure, enters the space in regions where the external suction is smaller than the internal suction. This will create an upstream flow underneath the cladding elements. If the flow resistance of this "internal flow" is increased, e. g. by decreasing the distance between cladding and building wall, or by producing a high flow resistance due to the supporting substructure, the internal pressure will be decreased in areas of small external pressures. For façades with rather small wind permeabilities the influence of the façade distance is negligeable since the flow resistance across the façade elements is much larger than the resistance of the internal flow.

Fig. 6 shows the plot of the largest net pressure coefficients taken from fig. 5 vs. the relative distance s/B. For the present study a relative distance s/B = 0,006 was chosen. For commonly used wind permeable façade coverings this distance will be much smaller (s/B ≤ 0,003). Therefore the results presented in this paper will be on the safe side.

The internal pressure distribution has been measured for all building models each being fitted with model façades with 5 different permeabilities. Fig. 7 shows a typical result, the external and internal pressure distribution along the long side of the building with the relative dimensions H/B = 0.5 and L/B = 2 for wind flow parallel to the long side. The upper diagram describes a situation where the fixation for the cladding elements and the battens which obstruct the internal flow has not

been considered. If the internal flow is blocked by impermeable battens the windload on the individual cladding elements will decrease greatly, see lower diagram of fig. 7.

3.2.3 Quasistatic windload on cladding elements

The quasi-static windload acting on a single cladding element corresponds to the difference of the time averaged external and internal pressures multiplied with the stagnation pressure of the design gust windspeed. For codification purposes the design windload has to be based on the largest net windload coefficient which can be taken from the pressure distribution. The largest net windlaod coefficients obtained from the windtunnel tests are summarized in the diagrams fig. 8, 9, 10, in which the largest net pressure coefficients measured for flow parallel to the considered façades are plotted vs. the relative height of the buildings H/B for the 3 different relative length L/B = 0.5; 1; and 2. The permeability coefficients considered cover the most important range of cladding systems used in practice. Again, the upper diagrams show the net windload coefficients for a building situation where no vertical battens are used, whereas the lower diagrams show the building situation for windtight vertical battens. As was already evident from fig. 7, there is a remarkable decrease in the windloading of cladding elements if the almost always necessary vertical battens are made airtight.

The beneficial effect of a large wind permeability of the façade coverings is most evident for very low-rise structures. The largest net windload coefficients on wind permeable façade coverings occur if the flow, which separates at the windward edges of the buildings, reattaches at the windparallel walls. Therefore the largest windloads on façade elements will occur on those building walls, where the external pressure distribution shows a distinct minimum. Since the largest negative pressure coeffi - cient for the external pressure and therefore the largest net windload coefficient has been measured for a building model with the relative dimensions L/B = 2 and H/B = 0.5, this model

was used to investigate the influence of different wind flow directions. Fig. 11 shows the results for façades with 4 different wind permeability coefficients C_D for flow direction $\alpha = -5°; +5°; +10°; +15°$. (Fig. 5 gives the equivalent diagran for $\alpha = 0°$.) In accordance with results presented by Frimberger (9) the highest external suction occurs at $\alpha \approx 10°$. For this flow direction the region of separated flow downstream of the windward edge of the buildings is relatively small, $l_s/L \approx 0.25$. Due to the small curvature radius of the stream lines off the separation region the suction at the building wall reaches a maximum.

Fig. 12 shows the results of similar investigations as described in fig. 11 for model façades with the various permeabilities investigated. The largest net windload coefficient is plotted vs. flow direction. For all permeabilities the ciritcal wind direction seems to be $\alpha \approx 10°$. Fig. 13 shows the net wind pressure coefficient for this flow direction plotted vs. the wind permeability, thus giving the design wind pressures which should be used for calculating the quasi-static windloads on permeable façade coverings on relatively low-rised buildings.

3.2.4 Windloads on cladding elements due to fluctuating pressures

To calculate the design windload for cladding elements a proper knowledge of the gust factors involved is necessary. The design windload for roofing elements is usually based on gust factors of 3 to 4. There is strong evidence that gust factors for building façades can far exceed this value (12). Vasanji and Gartshore (13) investigated the pressure fluctuation on a square cylinder spanning the whole width of the windtunnel. Maximum gust factors of slightly greater than 9 were observed. Frequency analyses of these pressure fluctuations showed a high energy content in a frequency range corresponding to reduced frequencies $nd/U = 0.3 \div 3$ (d = height of square cylinder).

The windload due to pressure fluctuations will not affect the cladding element if the time necessary for pressure equilibration between external and internal pressure is small compared to the gust time. Modifying an equation derived by Euteneuer (14) for calculating the time delay of the pressure equilibration process for buildings with openings, the frequency associated with the pressure equilibration process across cladding elements can be determined. Assuming an initial pressure differential of 1 000 Pa the pressure equilibration process for a large wind permeability ($C_D = 5{,}3 \cdot 10^3$) occurs corresponding to a frequency $n \approx 820$ Hz, for a small wind permeability ($C_D = 1{,}1 \cdot 10^6$) corresponding to a frequency $n \approx 60$ Hz. For a typical building with width B = 16 m and the design wind speed $U_\infty = 40$ m/s the largest reduced frequency with high energy content given by Vansanji and Gartshore corresponds to pressure fluctuation with n = 7,5 Hz. It may therefore be assumed that the cladding systems with rather small panels and rather large wind permeabilities thus far investigated will only experience the quasi-static windload given in the previous section.

4.0 Conclusions

1. The windload on permeable cladding elements is determined by the difference between external pressure distribution and the pressure distribution in the space between wind permeable cladding systems and wind impermeable building wall.

2. The resulting net windload may be significantly lower as compared to the windload on an impermeable façade.

3. To obtain small net windloads the flow resistance through the cladding system should be small, i. e. the cladding permeability should be large, and/or the internal flow resistance should be high.

4. Due to the rapid pressure equilibration across the permeable façade for cladding systems with small panels and large permeabilities only the quasi-static windload have to be considered.

5. To prevent pressure equilibration between adjacent walls of the building, which would increase the internal pressure and thus the net windload on cladding elements in critical wall regions, the edge connections have to be wind impermeable.

5.0 Acknowledgement

The cooperation and assistance of the ETERNIT AG, Berlin, during the investigations described in this report is gratefully acknowledged by the authors.

References

(1) T. Stathopoulos, D. Surry, A. G. Davenport:
A simplified model of wind pressure coefficients for low-rise buildings, in C. Kramer, H. J. Gerhardt (Eds.) Proc. 4th Colloquium on Industrial Aerodynamics, Building Aerodynamics, Part 1, pp 17 ff, Aachen (1980)

(2) C. Kramer, H. J. Gerhardt:
Windlasten auf Flachdächern, BundesBauBlatt 11 (1979) pp 496 ff

(3) C. Kramer, H. J. Gerhardt, S. Scherer:
Wind pressure on block-type buildings, in C. Kramer, H. J. Gerhardt (Eds.) Proc. 3rd Colloquium on Industrial Aerodynamics, Building Aerodynamics, Part 1, pp 241 ff, Aachen (1978)

(4) C. Kramer, H. J. Gerhardt, H.-W. Kuster:
On the windload mechanism of roofing elements, in C. Kramer, H. J. Gerhardt (Eds.) Proc. 3rd Colloquium on Industrial Aerodynamics, Building Aerodynamics, Part 3, pp 179 ff, Aachen (1978)

(5) R. A. Hazelwood:
The interaction of the principal wind forces on roof tiles, same ref. as (1), pp 119 ff

(6) C. Kramer, H. J. Gerhardt, H.-W. Kuster:
Windloads on surfaces of low-rise buildings, same ref. as (1), pp 33 ff

(7) R. P. Thorogood:
Resistance to air flow through external walls, BRE Information Paper IP 14/79 (1979)

(8) Chien et al.:
Wind tunnel studies of pressure distribution of elementary building forms, Iowa Institute of Hydraulic Research, State University of Iowa (1951)

(9) R. Frimberger:
Windkanalversuche zur Ermittlung von aerodynamischen Formbeiwerten für windparallele Gebäudewände prismatischer Baukörper, Forschungsbericht des Instituts für Strömungsmechanik der TU München, München (1979)

(10) D. Surry, A. G. Davenport, T. Stathopoulos:
Wind Loads on Low-Rise Structures, ASCE fall convention, Atlanta, Georgia (October 1979)

(11) P. E. Vermeulen, G. Th. Visser:
Determination of similarity criteria for windtunnel model testing of windflow patterns close to building façades, TNO-Bericht Nr. 79-06969/1p (July 1979)

(12) D. Surry, B. V. Tryggvason:
Fluctuating Pressures on Tall Buildings, Proc. 2nd US National Conf. Wind Engineering Research, (1975)

(13) Z. Vasanji, I. S. Gartshore:
Local pressure fluctuation on block structures, same ref. as (4), pp 153 ff

(14) G. A. Euteneuer:
Druckanstieg im Inneren von Gebäuden bei Windeinfall, Der Bauingenieur, Heft 6 (1970)

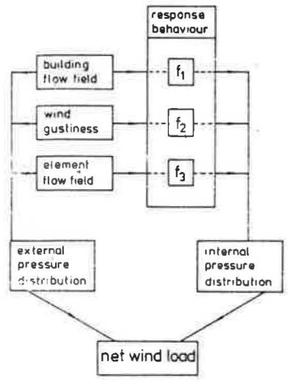

Fig. 1: Net windload of elements of permeable surface coverings as a difference of external and internal pressure distribution

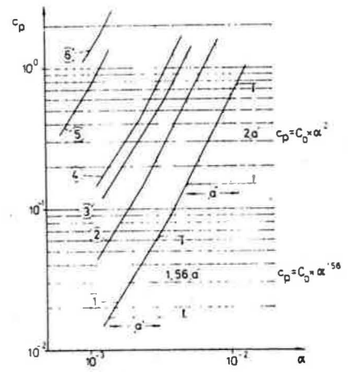

Fig. 2: Dimensionless pressure loss c_p vs. dimensionless volume flow α for flow through permeable façade coverings

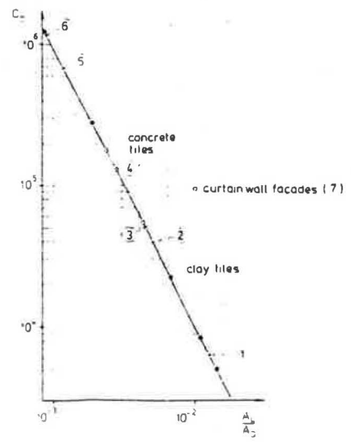

Fig. 3: Permeability factor C_D vs. percentage open area

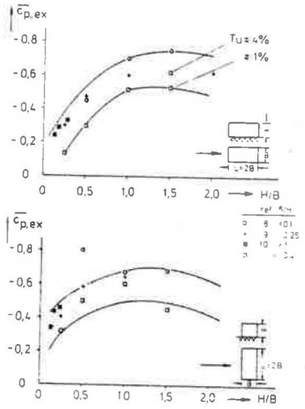

Fig. 4: Mean external wall pressure $\overline{c_{p,ex}}$ vs. relative buildings height H/B for sharp-edged buildings with rectangular plane form (L/B = 2)

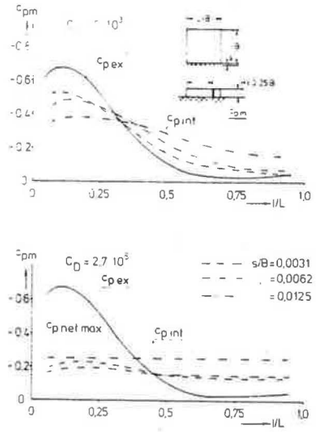

Fig. 5: External and internal pressure distribution for a typical low-rise building with permeable outer surface

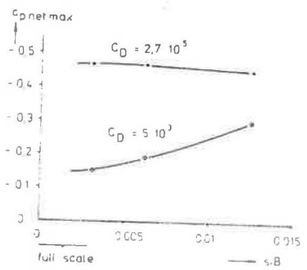

Fig. 6: Maximum net pressure coefficient $c_{p\ net\ max}$ vs. relative distance s/B

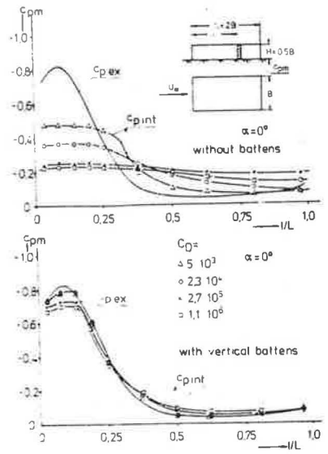

Fig. 7: External and internal pressure distribution for a typical building model

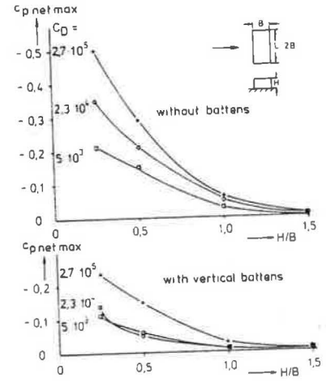

Fig. 8: Maximum net pressure coefficient $c_{p\ net\ max}$ vs. relative building height H/B for different wind permeability factors (L/B = 0.5)

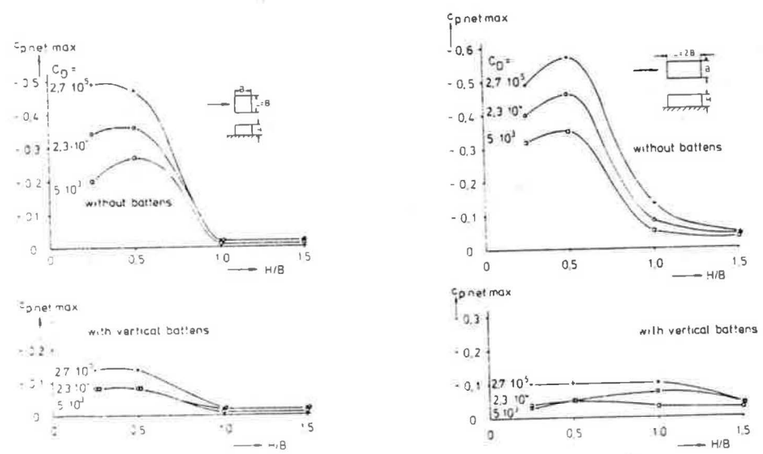

Fig. 9 and 10: Maximum net pressure coefficient $c_{p\ net\ max}$ vs. relative building height H/B for different wind permeability factors, L/B = 1 (9) and L/B = 2 (10)

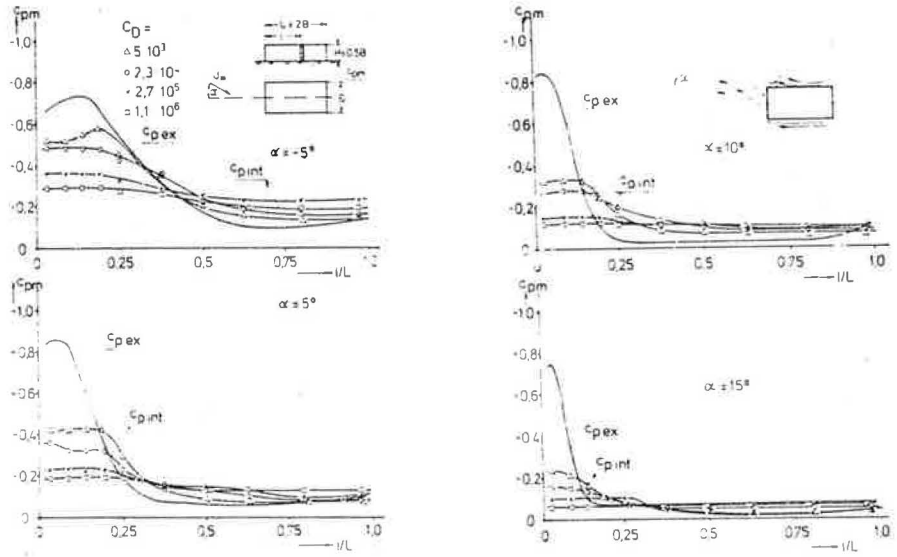

Fig. 11: Influence of wind flow direction on the external and internal pressure distribution for a building model with H/B = 0.5 and L/B = 2

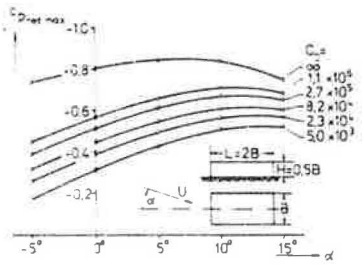

Fig. 12: Max. net pressure coefficient $c_{p\ net\ max}$ vs. flow direction α for a building model with H/B = 0.5 and L/B = 2

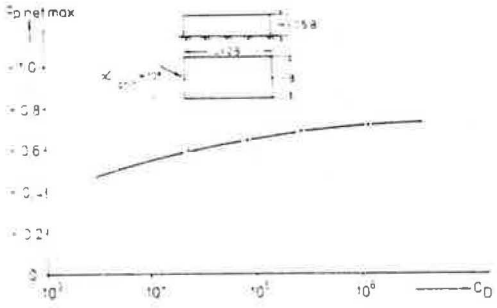

Fig. 13: Max. net pressure coefficient $c_{p\ net\ max}$ vs. permeability factor C_D for a building model with H/B = 0.5 and L/B = 2 and critical flow direction ($\alpha \approx 10°$)